

FAILURE ASSESSMENT OF CFRP SKINNED HONEYCOMB SANDWICH BEAM WITH DELAMINATION USING COHESIVE ZONE MODEL

Gopalakrishnan K C

Associate Professor, Department of Mechanical Engineering
College of Engineering, Trivandrum-695016, Kerala, India

Rameshkumar R

Head, Honeycomb Product Development Division, SDEG
Vikram Sarabhai Space Centre, Trivandrum, Kerala, India.

ABSTRACT

Cohesive zone model to capture the failure behaviour and strength of CFRP skinned cantilever sandwich beam with delamination is carried out and verified through test. The inputs required to represent the interfacial behaviour between the skin and honeycomb core in cohesive zone model are determined by standard tests. Acoustic emission was monitored during the test. Comparison of the load-displacement response obtained shows a good agreement with the experimental result. Both the test and analysis show a buckling induced delamination resulting earlier buckling failure of the specimen. Prediction of failure load based on nonlinear buckling analysis with CZM and without CZM approach shows a deviation of 6 % and 9% respectively with the test. The present study reveals that coupled buckling induced delamination failure of bonded sandwich structures can be accurately predicted by cohesive zone model which incorporates debond growth and buckling simultaneously. Parametric study reveals that the interfacial strength plays a key role in failure load of adhesively bonded sandwich structures in comparison to the delamination fracture toughness.

Keywords: Buckling induced debond growth, Carbon-Epoxy honeycomb sandwich, Cohesive zone modeling, Debond, Delamination, Double cantilever beam test.

Nomenclature

CZM	Cohesive zone model	G	Fracture Toughness
DCB	Double Cantilever Beam	σ_c	Interfacial Strength
AE	Acoustic Emission	δ	Interfacial Separation
FWT	Flat-wise Tension Test	F	Lamina Strength

1. INTRODUCTION

Composite honeycomb sandwich structures are widely used areas where high strength and light weight are the primary requirements. For the successful performance of these structures, the face-sheets and the core should be kept integral by the interface adhesive bond. A region, where there is no bond is called debond and in this region, the face-sheet will lose its support from the core and results in the loss of I-beam effect of the sandwich panel (Ahmed Abbadi, et.al, 2009). Due to in-service loading conditions, impact of foreign objects or high stress concentrations in the area of geometric and material discontinuities, the interface adhesive may be broken and lose the integrity between skin and core (Burman M,1998). Debonding leads to the reduction in strength of the structure. A reduction of 87% in load carrying capacity was observed for a 25mm through-width debonded structure in comparison to an undamaged sandwich structure reported by Aitken (2000). The behaviour of debonded sandwich structure is much more complex and the ability to predict the damage tolerance is one of the key factors to assess the margin of the sandwich structures.

It has been demonstrated analytically and experimentally that debond growth does not occur until the debond region has buckled and the growth is dominated by Mode I (peel) fracture (Han et al. 2002, Niu and Talreja 1999, Peck and Springer 1991). Whitcomb (1992) found that the peel stresses induced after buckling is the primary mechanism driving debond growth. The reduced buckling load due to the debond growth may be viewed as an endurance limit.

Interface debonding is generally very complex in nature and difficult to solve because it involves not only geometric and material discontinuities but also oscillatory singularity nature of the stress and displacement field in the vicinity of the debond tip (Rice, J. R. 1988, Alfano et al. 2007, Pirondi, A, and Nicoletto, 2000). The method of defining an initial crack and assuming self-similar progression of a crack as in traditional fracture mechanics approach becomes inefficient for modeling interface debonding (Ramesh Kumar, R, 2003, Camanho, P.P and Ambur, D.R, 2001). To circumvent the difficulties, by unifying strength-based crack initiation and fracture-based crack progression, the cohesive crack modeling approach has distinct advantages compared to other global methods (Needleman, A, 1987, 1990). This can be done by the use of special interfacial de-cohesion elements, placed between material layers or in the structure where cracking can occur (Kinloch, A.J, 1986). These elements introduce fracture mechanism by adopting softening relationships between tractions and the separations, which in turn introduce a critical fracture energy required to break apart the interface surfaces by combining a stress based and fracture mechanics based formulation. These elements are surface-like and are compatible with finite elements model of the structure (Prasad S, Carlsson LA. 1994).

The aim of the present study is to analyse, numerically and experimentally the failure process of debonded honeycomb sandwich cantilever beam, due to combined buckling and delamination growth and capture the failure load. In order to simulate numerically, non linear finite element analysis using 3-D CZM is followed. The interface between the core and skin is modeled using cohesive zone elements after experimentally obtaining the required parameters such as interfacial bond strength and mode-I fracture toughness (Shivakumar, K.N, Tan, J.C. Newman Jr., 1988). The load-displacement response of the beam is compared with the experimental result.

2. BUCKLING DRIVEN DELAMINATION

Debonded sandwich cantilever beams carrying transverse load, local buckling causes the debond growth (Fig.1) and thus the length of debond increases resulting in a greater reduction in load carrying capacity and experience a sudden failure. A large amount of research has been performed on this subject (Carlsson et al. 1991).

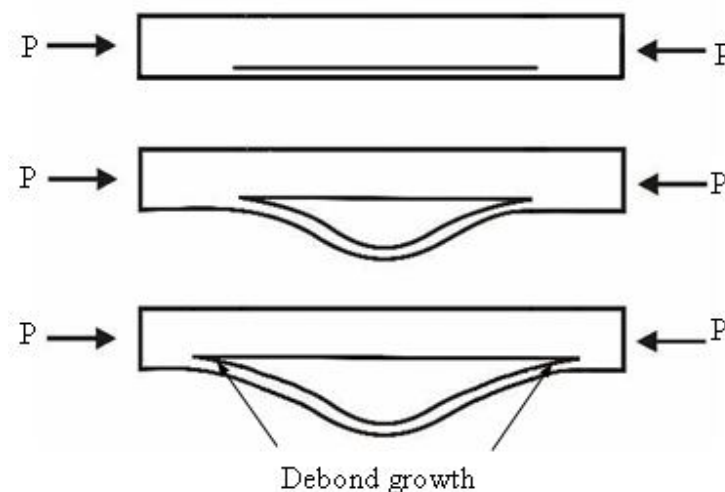


Fig.1 Buckling driven debond

Kardomateas(1993) studied the buckling and initial post buckling behavior of facesheet delamination or facesheet/core debond based on nonlinear beam theory with transverse shear deformation. Somers et al. (1991), Kim and Dharan (1992), and Hwu and Hu (1992) derived closed-form solutions of the critical buckling load. Chen et al. (1997) presented a continuous analysis to predict the local delamination buckling load of sandwich beams. Most of these previous analyses decouple the interaction between structural behavior and the fracture process, and thus can be used as a first order approximation for damage tolerance assessment (Tong-Seokhan, Ani Ural,2002). One way to couple the structural behavior and the fracture process is to use a cohesive zone model. The model was introduced to investigate the fracture process with nonlinear fracture mechanics.

3. COHESIVE ZONE MODELING (CZM)

The CZM is a damage mechanics model, able to describe the material behavior in the process zone ahead of a crack or delamination, was first envisaged by Needleman (1987, 1990). Basically it uses a traction-separation (T- δ) relation which correlates the stress (opening traction) and the displacement jump (crack face opening) in the process zone (Smith,1993, Chen.C.R et.al,2003). The idea of cohesive model is based on the consideration that infinite stresses at the crack tip are not realistic. CZM enables calculation of load for crack initiation and crack growth of ductile as well as brittle materials. The Dugdale-Barenblatt cohesive zone approach (Camanho, 2001, Blackman, 2003) served the theory for the decohesion elements used in FEM that incorporates the CZM damage mechanics. These elements use failure criteria that combine aspects of strength based analysis to predict the onset of the softening process at the interface and fracture mechanics to predict delamination propagation. An important advantage of decohesion elements is its capability to predict both onset and propagation of delamination.

In interface delamination and failure simulation, the structure on either sides of the bond is modeled as two separate regions and discretised such that the nodes in the interface have same coordinate values, but with different node numbers. A layer of decohesion elements of zero thickness is introduced in between the regions (Smith, 1993, Bin zhou, 2005). The cohesive zone represents a narrow band of localized deformation and is idealized as a pair of surfaces on which cohesive traction acts. The load displacement response of the cohesive zone is idealized by traction-separation law.

3.1. Exponential Traction Separation Law

According to Tvergaard (1992), delamination growth is associated with tractions across the interface that reaches a maximum value corresponding to the onset of delamination and then decreases gradually and finally vanishes when complete decohesion occurs (Tvergaard, V. and Hutchinson, J.W,1992,1996). The cohesive zone can still transfer load after delamination onset, until the critical value of the energy release rate is attained. In the present study this gradual decrease is represented as an exponential traction- separation (Volokh.Y,2004).

The exponential form of cohesive zone model (Needleman, 1987,1990, Youngseog Lee and Kwang Soo Kim,2002) uses a surface potential $\phi(\delta)$ as:

$$\phi(\delta) = e\sigma_{\max} \frac{\delta_n}{\delta_n} \left[1 - (1 + \Delta_n) e^{-\Delta_n} e^{-\Delta_n^2} \right] \quad (1)$$

where,

$$\Delta_n = \frac{\delta_n}{\delta_n} \quad (2)$$

$$\Delta_t = \frac{\delta_t}{\delta_t} \tag{3}$$

δ_n , δ_t and $\bar{\delta}_n$, $\bar{\delta}_t$ are the displacements and its peak values corresponding to opening and shear modes respectively. σ_{max} , the maximum normal traction at the interface is obtained from flat wise tension(FWT) test. It may be noted that for adhesively bonded joint, shear work of separation is same as normal work of separation

The normal and tangential traction forces T_n and T_t can be obtained by differentiating Eq. (1) w.r.t. δ_n and δ_t and are given as:

$$T_n = e\sigma_{max} \Delta_n e^{-\Delta_n} e^{-\Delta_t^2} \tag{4}$$

$$T_t = 2e\sigma_{max} \frac{\bar{\delta}_n}{\delta_t} \Delta_t (1 + \Delta_n) e^{-\Delta_n} e^{-\Delta_t^2} \tag{5}$$

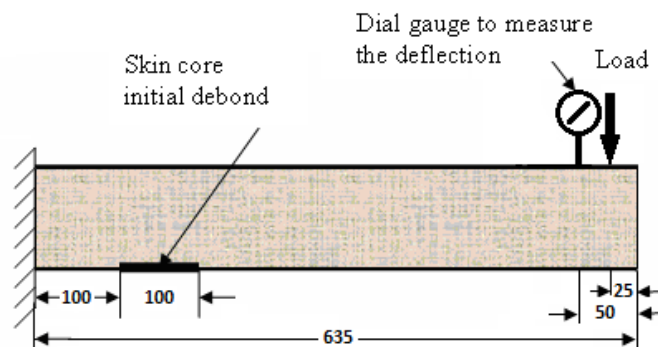
$$\phi_n = e\sigma_{max} \bar{\delta}_n \tag{6}$$

For pure mode I, normal work of separation, ϕ_n or G_{Ic} (J/mm² or N/mm) is obtained using Eq.1 by putting mode –II displacements to zero.

$$\phi_t = \sqrt{2e}\sigma_{max} \bar{\delta}_t \tag{7}$$

For pure mode II, shear work of separation, or G_{IIc} is obtained using Eq.1 by putting mode –I displacements to zero.

4. SPECIMEN DETAILS



Length - 635mm, Width - 95mm
Height - 41.6mm, Initial Debond -100mm

Fig.2 Debonded specimen

Table 1. Properties of the specimen

Material properties				
Skin		Honeycomb Core		
Skin - Carbon Epoxy laminate		Aluminium honeycomb core (AA 5056)		
Lay up	$(0^\circ,+45^\circ,-45^\circ,90^\circ)_S$	Density of the core	33 kg/m ³	
Ply thickness	0.1mm	Core height	40mm	
Skin thickness	0.8mm	Cell size of the core	6mm	
<u>Lamina Properties</u>		Foil Thickness of the core	$(1/1000)''$ - 0.0254mm	
E ₁	300GPa,	E ₂	6GPa	
ν_{12}	0.348,	G ₁₂	4.5GPa	
Tensile strength	F _{1T}	1600MPa	Modulus of elasticity	70GPa
Compressive strength	F _{1C}	1000MPa	Shear modulus in ribbon direction	
Tensile strength	F _{2T}	2MPa	G _{LZ}	230MPa
Compressive	F _{2C}	20MPa	Shear modulus in W direction	
Shear strength	F _S	75MPa	G _{WZ}	90MPa

5. EXPERIMENTAL METHODOLOGY

Honeycomb core is bonded to the cleaned carbon-epoxy face sheets of thickness 0.8mm using thin film adhesive (@0.1 mm after curing) and cured following well-known vacuum bag technique with negative pressure of one bar. Initial delamination was provided by Teflon sheet placed at the interface between the core and face sheet. Trimmed and sized specimens (Table.1, Fig.2, 3) are tested to ensure intact bond between core and skin by NDT (Fokker bond tester). Specimens are made in three sets as follows:

First specimen without debond is tested to validate finite element model wherein equivalent core properties are considered for comparison of load-deflection variation. Second specimen with debond is tested by providing delamination as shown in Fig.2, Fig.3and Fig.5. Then to fine tune the load close to the failure and to capture load displacement response, third specimen is tested up to failure.

6. FINITE ELEMENT ANALYSIS (CZM)

In CZM model (ANSYS software package), the honeycomb core is modeled as homogenized core and it's Young's modulus in thickness direction is obtained from the density ratio of honeycomb core and aluminium (Table.1). The carbon-epoxy skin, $(0^\circ,+45^\circ,-45^\circ,90^\circ)_S$ is modeled following overall orthotropic properties using eight node solid elements. Four node, zero thickness interface elements (inter-205) are introduced between the honeycomb core and skin except in the delaminated region of 100 mm as shown in Fig.2. To avoid interpenetration, contact is defined between the skin and core using elements conta174 and target170. One end of the beam is constrained for all degrees of freedom over a beam length of 30mm while the opposite end is loaded (25mm away from the tip as shown in Fig.2) using displacement control.

6.1 Evaluation of Delamination Fracture Toughness and Interfacial Normal Strength

In the case of aluminium skinned honeycomb sandwich, it is possible to obtain the delamination fracture toughness between the skin and core following the well-known drum peel test (ASTM standard D1781). Based on the available data bank, the lap shear strength coupon values for the same adhesive film used between CFRP skin to skin and aluminium skin to skin were found quite close to each other. Typically

the values were in the range of 17MPa to 20MPa. Hence drum peel test was carried out on aluminium coupons (for three numbers) of the same configuration (adhesive film, cell size, foil thickness, material for the core etc.) as that of the CFRP skinned sandwich used in the present study to determine the delamination fracture toughness and the same value is considered in this study. The interfacial normal strength required to CZM is evaluated by flatwise tension test (FWT) of bonded CFRP on aluminium core.

- a) Delamination fracture toughness, G_{Ic} - $460\text{J/m}^2 \pm 3\%$
- b) Interfacial tensile strength, σ_{max} - $3\text{MPa} \pm 2\%$ (based on FWT test)

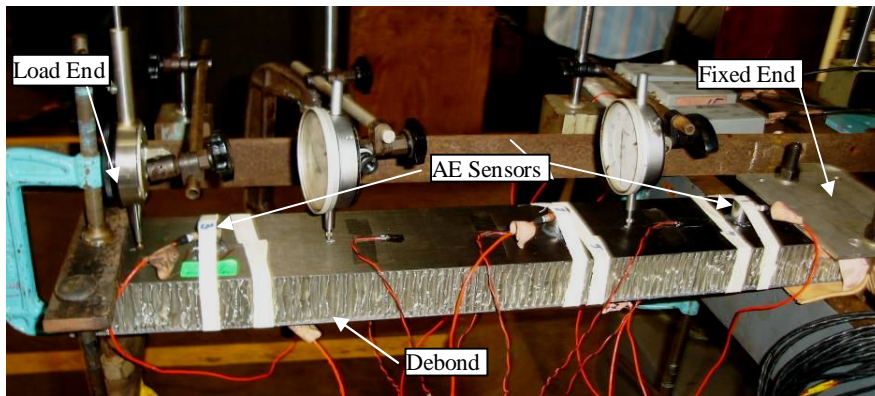


Fig.3 Experimental set-up for cantilever honeycomb sandwich beam with initial debond instrumented with AE sensors and dial gauges.

7. RESULTS and DISCUSSION

A nonlinear finite element analysis of CFRP skinned sandwich beam with debond (Fig.2) is carried out and captured the variation of load with displacement (at the loading point) using the CZM approach. To study the character of the debonded beam without considering the delamination growth, non linear buckling analysis is also conducted and buckling failure load is evaluated. Test was carried out by applying loads in steps at one end of sandwich beam (Fig.3) on a central hook and acoustic emission was monitored.

Initially, the load displacement character of the homogenized FEM model is verified and validated through test. AE was monitored to observe the honeycomb core crushing. A few AE signals were noticed at around 250N and the test was stopped. Then for the subsequent specimens, core was rigidised over 25 mm in the clamped end by drilling two pilot holes, resin was injected and cured at room temperature for 24 hrs and tested up to 300N. No AE signals were observed throughout the loading. Then the delaminated specimens were tested till failure and the load displacement variation is obtained. No honeycomb core crushing was noticed.

7.1 Test Results



Fig.4. Buckling failure and deformed configuration of the sandwich beam

While loading the carbon-epoxy skinned honeycomb sandwich beam with 100mm debond, up to 160N for a period of 1850s, only few AE signals were registered(Fig.5). The energy levels were very low. No AE signal was registered during the hold phases and thus ensured no delamination growth up to 160N. At 174N, a flood of higher amplitude AE signals are registered indicating the delamination growth and the specimen failed suddenly.

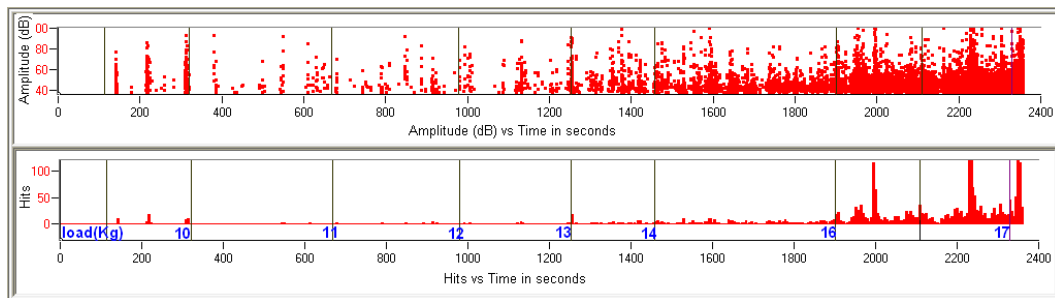


Fig.5. Acoustic Emission Data Monitoring of CFRP skinned sandwich beam

7.2 Post Test Observation

- 1) Debond region buckled outward as expected.
- 2) No Core crushing observed.
- 3) Comparison of NDT data carried out before and after the test revealed debond growth on either sides of the initial debond.
- 4) Fibre breakage of CFRP skin in the middle debond region noticed.
- 5) Acoustic data revealed the possible initiation of debond growth at 160N, followed by buckling of the skin and again a debond growth at 164.8N and then buckling and final fibre breakage of the skin in the debond region.

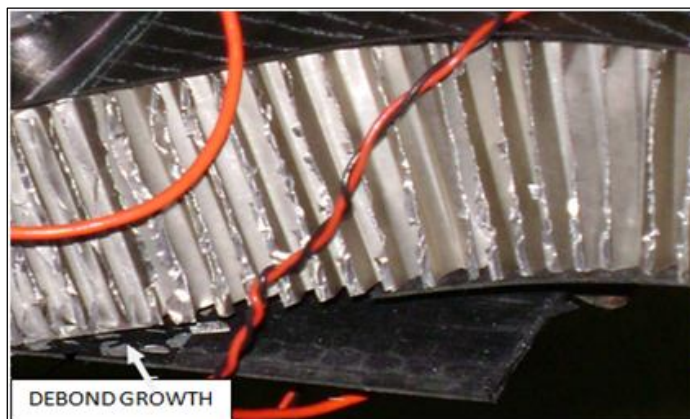


Fig.6 CFRP skinned sandwich specimen showing debond growth and breakage of the skin through the width

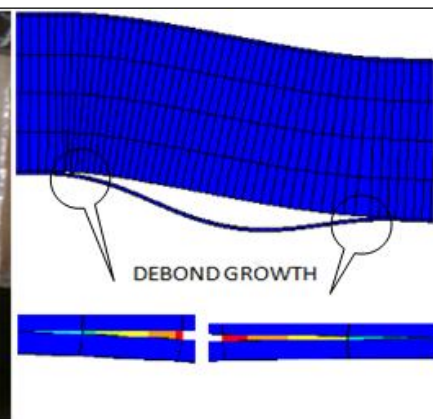


Fig.7 FEA model showing debond Growth on both sides of the skin through the width

7.3 Comparison between the test and analysis results

Non linear finite element analysis using CZM model gives a peak load of 170N and an ultimate failure load of 158N (Fig.8) as against the test results of 174 N. Test did not show a much difference between the peak and ultimate failure loads as there was a sudden collapse of the beam with fibre breakage in the middle of the debond region just after the peak load. Since the mode of failure was fibre breakage, average CFRP skin stresses (overall orthotropic property only possible to consider) on the tensile and compressive region are obtained as shown in Fig.9. The inner region of the debond skin experiences a compressive stress and the value reaches to the compressive strength of the skin (353MPa) when the tip load reaches 164N (Fig.9). Outer fibre of the debond region experiences a stress of 365MPa as against its tensile strength of 370MPa. Hence based on the compressive strength, the failure load is evaluated as 164N and this result shows a variation of 6% with test data. In nonlinear buckling analysis without considering the debond growth, fibre breakage occurs at 190N and this load shows a variation of 9% with test data while the buckling instability was noticed at 234N when the fibre breakage was ignored.

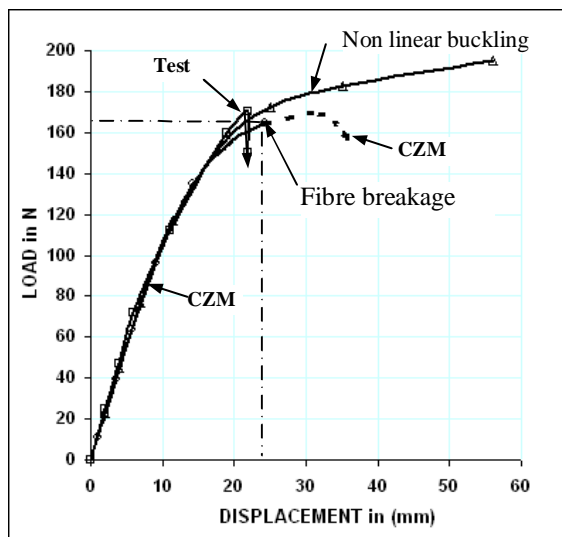


Fig.8 Load Displacement Response of the Specimen

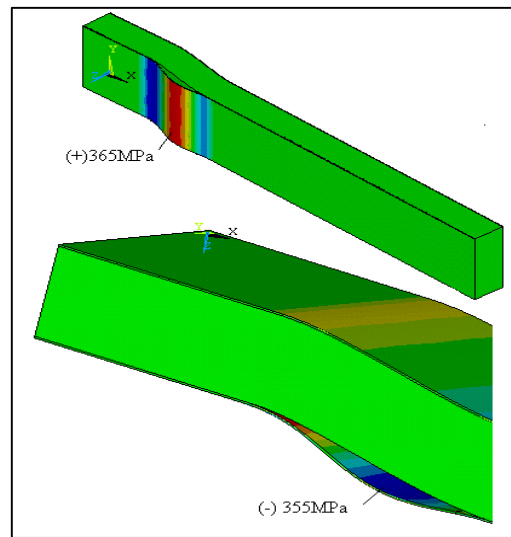


Fig.9 Maximum stress at the outer and inner faces of the debond skin corresponding to 164N

Table-2 Comparison of failure load by test and analysis

	Buckling analysis without CZM	Test (average of two)	CZM
			Load at fibre breakage
Peak load	190N	174N	164N
Variation with Experimental result	9%		6%
Delamination growth (Fig. 7)		10.3mm(Left) 12.2 mm(Right)	5mm (Left) 10mm (Right)
Delamination Crack tip opening			0.3mm (Left) 1.2mm (Right)

7.4 Parametric Study

Parametric study is conducted by using CZM to study the effect of interfacial fracture toughness and normal strength on the residual strength of the delaminated specimen. Analysis has done for various interfacial strength values while keeping the fracture toughness value constant Fig.10(a). The load carrying capacity of the specimen increases with increase in interfacial normal strength and observed a linear relationship between the two. Fig.10(b) shows the effect of fracture toughness on peak load while keeping the interfacial strength value constant. It is observed that for lower values of fracture toughness, there is less increase in failure load but for higher values of fracture toughness there is significant increase in failure load. Fig.10(b) also shows that for higher values of interfacial strength, effect of fracture toughness on failure load goes on reducing.

This study reveals that, buckling induced debond growth causes the early failure of sandwich structures and the failure load and failure mechanism are mainly controlled by interfacial strength value of the adhesive.

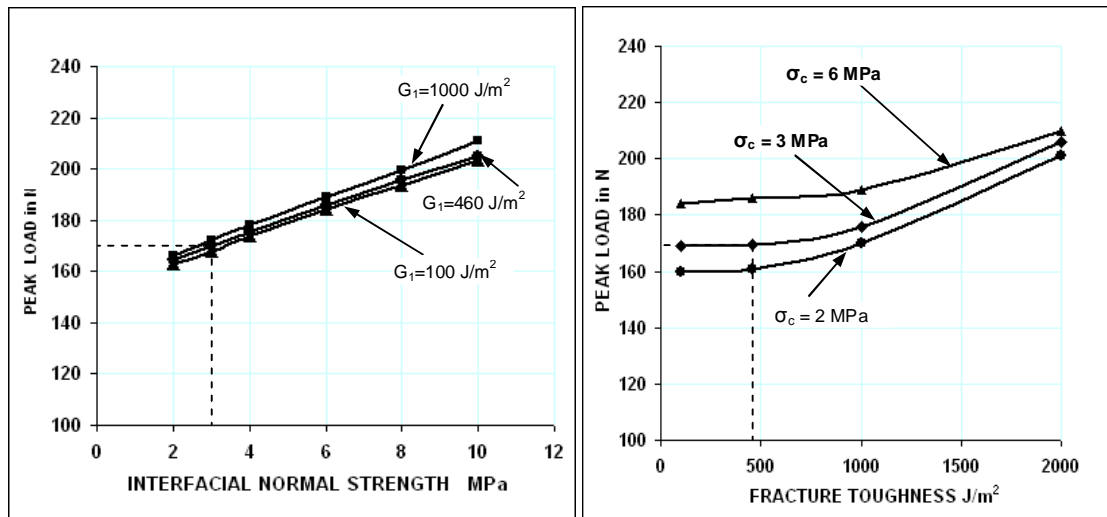


Fig.10(a)Effect of interfacial strength on peak failure load of the specimen

Fig.10(b) Effect of Fracture toughness on peak failure load of the specimen

8. CONCLUSIONS

A nonlinear finite element analysis of CFRP skinned honeycomb sandwich beam with debond has been carried out by cohesive zone model, introducing interface cohesive zone elements between the skin and core and is validated by test. A coupled delamination - buckling has been evidenced from both CZM approach and test. The load displacement response from CSM shows a good agreement with the test. Load corresponding to the fibre breakage failure followed by delamination induced buckling is captured in CZM by comparing the skin stress and skin strength and shows only 6% variation. Non linear buckling analysis without simulating debond growth also carried out and the failure load due to fibre breakage shows a variation of 9% with test.

Based on the parametric study, the effect of interfacial bond strength and delamination fracture toughness on the failure load, it is concluded that buckling induced debond growth causes the early failure of sandwich structures and the failure load is mainly controlled by interfacial strength value of the adhesive.

REFERENCES

1. Ahmed Abbadi A, Koutsawa Y, Carmasol A, Belouettar S, Azari Z(2009) Experimental and numerical characterization of honeycomb sandwich composite panels, *Simulation Modelling Practice and Theory*, 1533-1547.
2. Aitken R R (2000) Damage due to soft body impact on composite sandwich aircraft Panels, *PhD thesis The University of Auckland, New Zealand*.
3. Alfano, Furgiuele, Leonardi, Maletta, Paulino G H(2007) Fracture analysis of adhesive Joints using intrinsic cohesive zone models, *Key Eng Ma,t* 348, 13-16
4. Bin zhou M.D, Tthouless and Ward S.M. (2005)Determining mode-I cohesive parameters for fracture in ultrasonic spot welds, *International Journal of Fracture*,136:309-326
5. Blackman. B.R.K, Hadavinia.H(2003) The use of cohesive zone model to study the fracture of fiber composites and adhesively bonded joints, *International Journal of Fracture*, 119:25-46
6. Burman, M. (1998) Fatigue crack initiation and propagation in sandwich structures. *PhD thesis, Royal Institute of Technology, Sweden*.
7. Camanho.P.P, Davila.C.G and Ambur.D.R(2001)Numerical Simulation of Delamination Growth in Composite Materials, *NASA/TP-2001-211041*
8. Carlsson L A, Sendlein L S and Merry SL(1991) Characterization of face sheet/core shear fracture of composite sandwich beams, *Journal of Composite materials*, 25:101- 116.
9. Carlsson LA (1991)On the design of the cracked sandwich beam (CSB) specimen, *Journal of Reinforced Plastics and Composites*,10: 434-444
10. Chen S H, Lin C C and Wang J T S (1997) Local buckling of delaminated sandwich beams using continuous analysis, *International Journal of Solids and Structures*,34:275-288
11. Chen C R, Kolednik I, Scheider T(2003) On the determination of the cohesive zone parameters for the modeling of micro-ductile crack growth in thick specimens, *International Journal of Fracture*, 120: 517–536
12. Han T, Ural A, Chen C-S, Zehnder AT, Ingraffea AR, Billington SL (2002) Delamination buckling and propagation analysis of honeycomb panels using a cohesive element approach, *International Journal of Fracture*,115: 101-123
13. Hwu C and Hu J.S. (1992) Buckling and postbuckling of delaminated composite sandwich beams, *AIAA Journal*, 30: 1901-1909
14. Kardomateas G A (1993) The initial post-buckling and growth behavior of internal delaminations in composite plates, *Journal of Applied Mechanics*, 60:903-910
15. Kinloch A J (1986) Adhesion and Adhesives Chapman and Hall, London, UK
16. Kim W C and Dharan CKH (1992) Facesheet debonding criteria for composite sandwich panels under in - plane compression, *Engineering Fracture Mechanics*, 42: 643-652.
17. Needleman A(1990) An analysis of decohesion along an imperfect interface, *International Journal of Fracture*, 42: 21–40.
18. Needleman A(1987)A continuum model for void nucleation by inclusion debonding, *Journal of Applied Mechanics*, 54:525-531.
19. Niu K Talreja R(1999) Buckling of a thin face layer on winkler foundation with Debonds, *Journal of Sandwich Structures and Materials*, 1: 259-278
20. Pironi A and Nicoletto(2000), *Proceedings of the XV Congress of Italia Group of Fracture (IGF) Bari, Italy*
21. Peck S O Springer G S (1991) The behaviour of delaminations in composite plates- analytical and experimental results, *Journal of Composite Materia,s*, 25:907-925
22. Prasad S, Carlsson LA(1994) Debonding and crack kinking in foam core sandwich beams-experimental investigation, *Eng Fract Mech*, 47:825–41
23. Ramesh Kumar R, Praveen K S and Venkateswara Rao(2003) Assessment of Delamination Fracture Load of Stringer Stiffened Composite Panel, *AIAA Journal*, 3: 551- 553
24. Rice J R (1988) Elastic fracture-mechanics concepts for interfacial cracks, *J. App.Mechs*, 55:98-103
25. Somers M, Weller T and Abramovich H (1991) Influence of predetermined delaminations on buckling and postbuckling behavior of composite sandwich beams, *Composite Structures*, 17: 295–329

26. Smith E (1993) A collection of useful formulae for cohesive zone Parameters, *International Journal of Fracture*, 64:37-43
27. Shivakumar K N, Tan J C, Newman Jr.(1988) A virtual crack-closure technique for calculating stress intensity factors for cracked three dimensional bodies, *Int.J.Fract.*,36:43-R50
28. Tong-Seokhan, Ani Ural(2002) Delamination buckling and propagation analysis of honeycomb panels using a cohesive element approach, *International Journal of Fracture*, 115:101-123
29. Tvergaard V and Hutchinson JW (1992) The relation between crack growth resistance and fracture process parameters in elastic-plastic solids, *Journal of the Mechanics of Solids*, 40:1377-1397
30. Tvergaard V and Hutchinson J W(1996) Effect of strain-dependent cohesive zone model on prediction of crack growth resistance, *International Journal of Solids and Structures*, 33: 3297-3308
31. Volokh Y(2004) Comparison between cohesive zone models, *Communications in Numerical methods in Engineering*
32. Whitcomb J D (1992) Analysis of a laminate with a postbuckled embedded delamination - including contact effects, *Journal of Composite Materials*, 26:1523-1534
33. Youngseog Lee and Kwang Soo Kim(2002) A Cohesive surface separation potential, *KSME International Journal*, 16:1435-1439